Organometallic "super reducing agents". Electron transfer chemistry of photogenerated 19e⁻ W(CO)₅(L)⁻· radicals[1]

Igor S. Zavarine, Clifford P. Kubiak *

Purdue University, Department of Chemistry, 1393 Brown Laboratory, West Lafayette, IN 47907-1393, USA

Received 15 August 1997; accepted 19 November 1997

Contents

Abstract

The existence of "19-valence electron radicals" has been a controversial issue in organometallic chemistry. The premise that photochemical excitation of $[W_2(CO)_{10}]^{2-}$ in the presence of donor solvents or phosphine ligands (L = THF, MeCN, 2-methyl THF, PEt₃) leads to highly reducing 19e⁻ L–W(CO)₅⁻· radicals was investigated by laser transient absorption (TA) spectroscopy in the UV–vis and IR regions and by electron transfer kinetics studies. Infrared transient absorption measurements were found to be well suited to the $[W_2(CO)_{10}]^{2-}$ system. The IR transient absorption spectrum at < 1 μs following the laser

* Corresponding author. Fax: +1 317 494 0239.
[1] Dedicated to the memory of Professor Jeremy K. Burdett.

pulse in THF and MeCN is dominated by new IR absorptions at $v(CO) > 1960$ cm^{-1}. The IR transient absorption spectrum at > 10 μs following the laser pulse is dominated by IR absorptions at $v(CO) = 1860$ and 1816 cm^{-1}. The significant lowering of $v(CO)$ energy in the first 10 μs is assigned to a 19e$^-$ solvent–W(CO)$_5^-$ (solvent = MeCN, THF) radical. Rate constants for second order recombination (k_r) of these radicals are strongly solvent dependent. A homologous series of substituted benzophenone electron acceptors (A) with $E_{1/2}$ (A/A$^-$) ranging from -1.21 to -2.26 V vs. SCE were chosen to study the electron transfer chemistry of the 19e$^-$ species in THF. Electron transfer rate constants (k_{et}) were found to range from 4×10^4 M^{-1} s^{-1} for reduction of the least energetically favorable acceptor (cyclohexylphenyl-ketone, $E_{1/2} = -2.26$ V vs. SCE) up to 8×10^8 M^{-1} s^{-1} for reduction of the most energetically favorable acceptor (decaflurobenzophenone, $E_{1/2} = -1.21$ V vs SCE). The data were interpreted within the context of the Marcus theory of electron transfer. The abnormally large total reorganization energy, $\lambda = 70$ kcal mol^{-1}, and slow derived self-exchange rate constant, $k_{11} < 1$ M^{-1} s^{-1}, reflect the large nuclear displacements associated with the 18e$^-$/19e$^-$ couple. It is concluded that although the 19e$^-$ solvent–W(CO)$_5^-$ radicals are thermodynamically "super reducing agents", capable in principle of single electron transfers to a wide variety of substrates, they are kinetically incompetent due to the enormous reorganization energy required to accommodate the nineteenth electron. © 1998 Elsevier Science S.A.

1. Introduction

The proposed existence of "19-valence electron radicals" has been a controversial issue in organometallic photochemistry [1–6]. Tyler reported the photochemistry of transition metal carbonyl dimers in the presence of electron pair donor ligands [7–9]. Photochemical dπ–σ* or σ–σ* homolysis of the metal–metal bonds results in the formation of a pair of 17-valence electron organometallic radicals. In the presence of electron pair donor ligands, the 17-valence electron radicals were proposed to form 19-valence electron adducts. The evidence for the 19-valence electron adducts was largely inferential, based on the formation of powerful reducing equivalents when photochemical metal–metal bond homolysis was effected in the presence of donor ligands.

It is important at the outset to distinguish between genuine 19e$^-$ radicals, those organometallic radicals having an electron localized in a metal–ligand antibonding orbital, and other types of 19e$^-$ adducts. For example, cyclopentadienyl ring slippage from η^5 to η^4 in Fe(CO)$_3$(CpCH$_2$Ph) can lead to a stable 18e$^-$ compound [10], which without recognition of the ring slip might otherwise be considered as a 19e$^-$ species. In other cases the nineteenth electron is localized in a low energy ligand-based orbital, much like a metal to ligand charge transfer (MLCT) state. The species Mo(CO)$_4$(bpy$^{\cdot-}$) is an example of such a ligand-centered radical [11]. These ligand-centered radicals are considered to be $18 + \delta$ e$^-$ species, where the δ e$^-$ is understood to not be included in the valence shell of the metal. While so called $18 + \delta$ e$^-$ radicals have been characterized spectroscopically by EPR [12], Mossbauer spectroscopy [2,13], and in some cases by X-ray crystallography [14], there is no *direct* spectroscopic evidence for the existence of genuine 19e$^-$ radicals. The sole
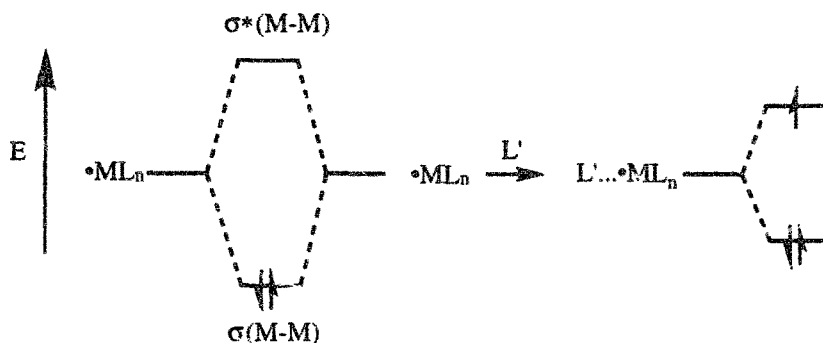
Scheme 1. Energetics of formation of 19 electron radicals

report of an investigation of the supposed formation of $19e^-$ transient species by time resolved infrared spectroscopy (TRIRs) failed to find evidence of the formation of these intermediates [15]. One thing is certain: if formed, $19e^-$ species would be tremendously potent reducing agents. Indeed, the experimentally determined ionization potentials of some of the $19e^-$ compounds are close to that of potassium metal [2,16]. The formation and energetics of the proposed $19e^-$ radicals are considered in Scheme 1.

The driving force for the formation of the $19e^-$ $L'-ML_n^-$ radical in simplest terms is half the bond energy, BE (M–L'), of the new metal–ligand bond [1,17]. It is important to note that a $17e^-$ ML_n^- radical is already a powerful reducing agent. Any radical formed by bond homolysis is simultaneously a more powerful reducing agent and a more powerful oxidizing agent compared to the ground state bonded species, by a potential energy difference approximately equal to the bond dissociation energy. The "super" reducing potential of a $19e^-$ $L'-ML_n^-$ radical is a consequence of the electronic destabilization of the unpaired electron (by an energy of approximately BE (M–L')) since this electron is now formally assigned to the σ^* (M–L') orbital resulting from the new metal–ligand bond.

Here we describe our studies of the photochemistry of $[W_2(CO)_{10}]^{2-}$ in the presence of donor solvents and phosphine ligands (L = THF, MeCN, 2-methyl THF, PEt_3) using laser transient absorption spectroscopy in the UV–vis and IR regions. We also describe electron transfer kinetics studies of the photogenerated tungsten radical transients. We show how these spectroscopic observations and Marcus interpretation [18,19] of the kinetics of electron transfer point to the existence of $19e^-$ $L-W(CO)_5^-$ radicals.

2. Experimental section

2.1. Materials

All solvents were dried using appropriate agents. Tetrahydrofuran (Fisher), and 2-methyltetrahydrofuran (Aldrich) were distilled from the sodium benzophenone

ketyl. Acetonitrile (Fisher) was distilled from the CaH_2. Hexanes and diethyl either were HPLC grade. All solutions were used fresh and all manipulations were done in the dry box under rigorously dry and oxygen-free atmosphere. Decafluorobenzophenone, 3-nitrobenzophenone, 2-amino-5-nitrobenzophenone, 3,3'-bis(trifluoromethyl)benzophenone, 2,3,4,5,6-pentafluorobenzophenone, 4,4'-dichlorobenzophenone, benzophenone, 4-aminobenzophenone, 4,4'-dimethoxy-benzophenone, 4,4'-bis(diethylamino)benzophenone, cyclohexylphenylketone, triethylphosphine, tributylphosphine and triphenylphosphine were all obtained from Aldrich and used as received. TBAH (tetrabutylammonium hexafluorophosphate) was received from Aldrich, recrystallized from hot dry ethanol and dried in vacuo at 170 °C for 48 h. Tungsten hexacarbonyl (Aldrich) was sublimed at 40 °C prior to use. 2,2'-Bipyridine was recrystallized from THF. $Na_2[W_2(CO)_{10}]$ was prepared by a procedure analogous to that by Tyler et al. [7]. $W(CO)_5(THF)$ was prepared by irradiation by UV light of $W(CO)_6$ in THF as a solvent.

2.2. Preparation of [PPN]₂[W₂(CO)₁₀]

The bis(diphenylphosphino) iminium salt, $[PPN]_2[W_2(CO)_{10}]$, was prepared by cation exchange. 0.490 g of $Na_2[W_2(CO)_{10}]$ in a minimum amount of acetonitrile (ca. 1 mL) was added to 0.844 g (5% excess) of PPNCl (Aldrich) also in minimum amount of acetonitrile (ca. 0.7 mL). After 2 h, a white precipitate of NaCl was filtered. 50 mL of hexanes and 50 mL of diethyl either were added to precipitate $[PPN]_2[W_2(CO)_{10}]$. This was washed on a filter frit with a small amount of THF and 50 mL of hexanes. Yield: 0.84 g (69%) as an orange-yellow crystalline product.

2.3. Laser flash photolysis

The UV–vis laser flash photolysis system employed uses the third ($\lambda = 355$ nm) harmonic of a Continuum Nd:YAG (Model NY-60) laser as a pump for a dye laser (Continuum, ND-60) with Coumarin 420 (Exciton) used as a dye. Laser pulse energies varied from 5 to 200 mJ/pulse. The excitation and the probe beam cross at 90°. The pathlength was 4 mm for the excitation beam and 10 mm for the probe beam. An arc lamp (PTI) served as the source of the probe radiation. Its broadband output was passed through an 8-cm long water filter to remove infrared and short wavelength UV radiation, then focused by a cylindrical lens onto the monochromator (Oriel) and passed through a flow cell (Starna F-49) containing the sample. Transient absorption changes were measured through a second monochromator coupled to a photomultiplier tube (Hamamatsu R446). The contents of the flow cell were refreshed with a syringe pump. A Fisher syringe pump outfitted with gas-tight Teflon or Kel-F tubing, valves and syringes (Hamilton) were used for precise and continuous flow rate regulation. Each kinetic trace recorded was averaged with up to 50 other traces.

Some transient absorption data were obtained using a lens-intensified charge-coupled device (ICCD). A Princeton Instruments CCD detector with the Princeton

Instruments programmable pulse generator (PG-200) fitted to an Action Research Corporation Spectra Pro-275 spectrograph were used. The 300–600 nm region of the spectrum could be covered with this instrument with time resolution of 5 ns, and the transient absorption spectra were obtained after various specific delay times.

Transient IR data were obtained on a system based on either an InSb or MCT detector. The output from a Nernst globar source was collected by a parabolic mirror, focused by a CaF_2 ($f = 6$ in.) lens, then focused through another CaF_2 lens ($f = 2$ in.) onto the detector. The system was a modified version of that reported by Grant for gas phase transient IR absorption experiments [20,21]. Modifications to the system used in this study for liquid samples include the use of the third harmonic ($\lambda = 355$ nm) output of a Nd:YAG laser. A liquid flow cell was used based on a standard IR liquid cell connected to a syringe pump. The IR beam and the excitation source crossed in the cell at an angle of *ca.* 5°. Typical pathlengths were 0.2–0.5 mm, and typical sample concentrations were 5×10^{-4} M.

2.4. Cyclic voltammetry

A Princeton Applied Research model 173 potentiostat and EG&G PARC model 175 programmer were used with the output connected to an XY plotter or a digital oscilloscope (LeCroy 9400A). A gold electrode (BAS) or gold microelectrode (BAS) (with diameters 2.5 or 10 μm) were used as working electrodes. Platinum wire served as the counter electrode and a 1:1 ferrocene/ferrocenium hexafluorophosphate couple in acetonitrile served as a reference. For all measurements (especially in THF) the solution resistance was carefully iR compensated. Since many of the benzophenone derivatives studied exhibit irreversible electrochemistry at normal scan rates (up to 1 V s^{-1}), faster scan (up to 100 V s^{-1}) microelectrode techniques were employed to obtain the $E_{1/2}$ values appearing in Table 1 under electrochemically reversible conditions.

3. Results and discussion

3.1. Flash photolysis of $Na_2[W_2(CO)_{10}]$

Laser induced dπ–σ^* or σ–σ^* excitation of $Na_2[W_2(CO)_{10}]$ in MeCN or THF results in the prompt formation of $W(CO)_5^{-}$ radicals. At 472 nm, an instantaneous increase in absorption is observed which then decays by an apparent second order process over several milliseconds. The dπ–σ^* absorption due to $[W_2(CO)_{10}]^{2-}$ at 430 nm is simultaneously bleached by laser excitation, and then restored on the same time scale. Infrared transient absorption measurements have proven to be particularly suitable for the $[W_2(CO)_{10}]^{2-}$ system. In acetonitrile solutions, $[W_2(CO)_{10}]^{2-}$ exhibits $\nu(CO)$ bands at 1941(m), 1891(vs) and 1790(s) cm^{-1}. Laser excitation produces an instantaneous bleaching of IR absorption at 1940, 1887 and 1790 cm^{-1}, which is then restored. The response monitored at 1887 cm^{-1} is shown in Fig. 1. Coupled to the disappearance of $[W_2(CO)_{10}]^{2-}$ is an appearance and decay
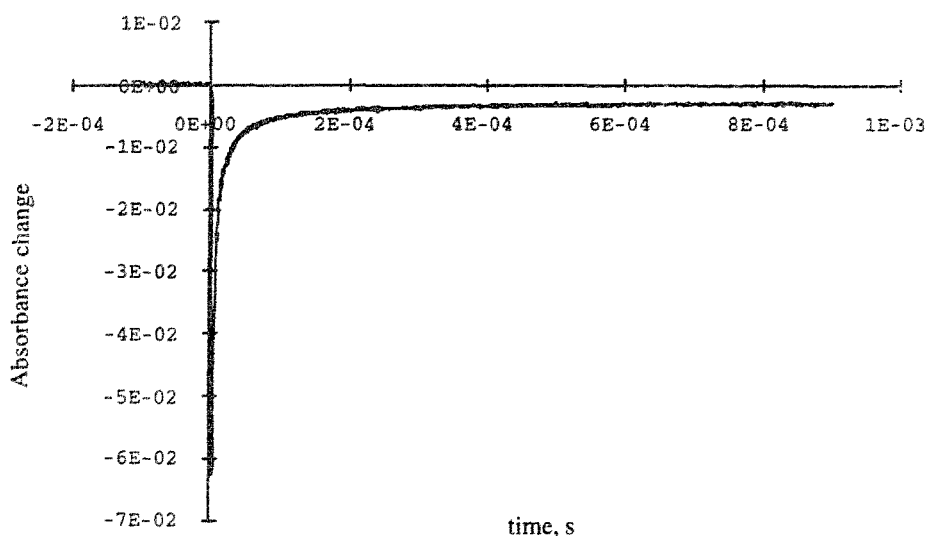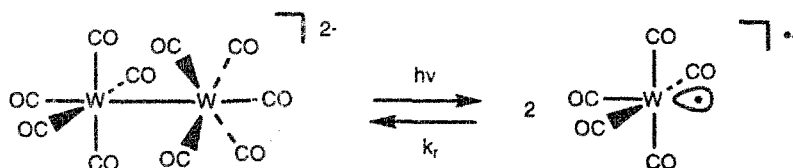
Fig. 1. Transient disappearance and reformation of the $[W_2(CO)_{10}]^{2-}$ species in THF. $\lambda_{excitation} = 355$ nm and $\lambda_{observation} = 1887$ cm^{-1}.

of IR absorbance at 1851 cm^{-1}, Fig. 2. These observations are as expected for photochemical metal–metal bond homolysis, followed by radical–radical recombination, Eq. (1).

The disappearance of $W(CO)_5^-$ radicals follows second order kinetics, as observed by either UV–vis or IR. The radical–radical recombination rate constant, k_r, can be calculated from the transient decay observed at 472 nm at 3×10^9 M^{-1} s^{-1}. The extinction coefficient of $W(CO)_5^-$ radicals at 472 nm is estimated as $\epsilon_{472}[W(CO)_5^-] = 2 \times 10^3$ M^{-1} cm^{-1}. IR transient absorption data give essentially the same rate constant for the radical recombination process. The IR extinction coefficient of $W(CO)_5^-$ radicals at 1860 cm^{-1} is enormous and was estimated as $\epsilon_{1860}[W(CO)_5^-] = 1 \times 10^4$ M^{-1} cm^{-1}.

The generally excellent agreement in the values of the second order recombination rate constants calculated from the disappearance of $W(CO)_5^-$ radicals k_r (at 472 nm) $= 3 \times 10^9$ M^{-1} s^{-1} and the reappearance of $[W_2(CO)_{10}]^{2-}$ k_r (at 350 nm) $= 4 \times 10^9$ M^{-1} s^{-1} confirms the idea that irradiation of $[W_2(CO)_{10}]^{2-}$ leads to metal–metal bond homolysis, followed by second order recombination of $W(CO)_5^-$ radicals. We note that these rate constants were calculated assuming negligible absorbance of the $W(CO)_5^-$ radicals below 370 nm.

The diffusion-controlled rate constant in CH$_3$CN for an uncharged species is
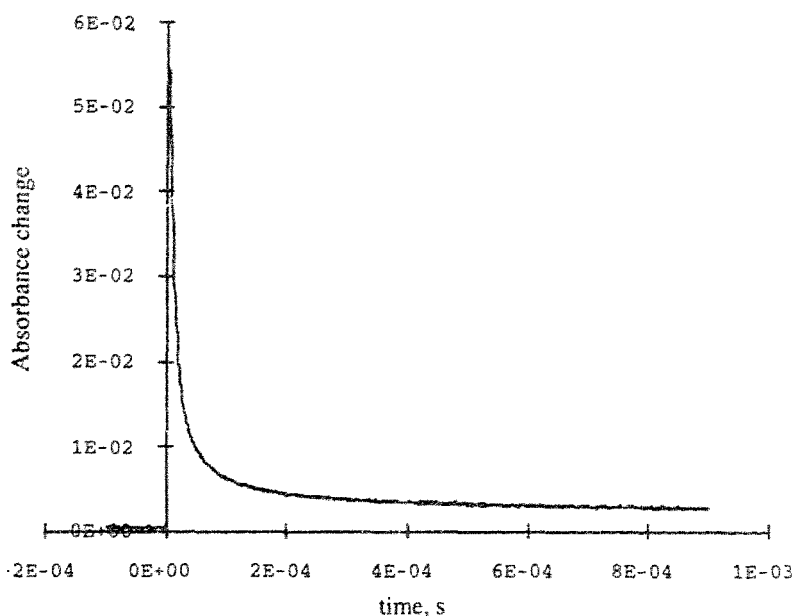
Fig. 2. Transient absorption appearance and decay of $W(CO)_5^-$ in THF: $\lambda_{excitation} = 355$ nm and $\lambda_{observation} = 1851$ cm^{-1}.

$k_{dc} = 3 \times 10^{10}$ M^{-1} s^{-1} [22]. For spin-statistical reasons, the rate constant for the recombination of two $S = 1/2$ radicals is $1/4$ of that for singlet species, or 7×10^9 M^{-1} s^{-1}. The corrected form of the von Smoluchowski equation, when the reacting partners are ions, is given by Eqs. (2) and (3) where ϵ is the dielectric constant of the solvent, ϵ^0 is permitivity of vacuum, k_B is the Boltzmann constant and r_{AB} is the radius of the molecule.

$$k_{dc} = k_{dc}(\text{neutral})^* f \tag{2}$$

$$f = \frac{\delta}{e^{\delta} - 1} \text{ where } \delta = \frac{z_a z_b e^2}{(4\pi\epsilon^0)\epsilon k_B T r_{AB}} \tag{3}$$

If the radius of the $W(CO)_5^-$ anion is taken as a sum of the W–C and C–O bond lengths, or 4 Å, then the corrected value of k_{dc} is 2×10^9 M^{-1} s^{-1}, which is close to our experimental values within experimental error. Hence, $W(CO)_5^-$ radical recombination is essentially diffusion-controlled in acetonitrile.

However, the decay of the transient $W(CO)_5^-$ and reappearance of $[W_2(CO)_{10}]^{2-}$ absorptions, shown in Fig. 2, can be seen to be incomplete on the millisecond time scale (both by IR or UV–vis). Complete recovery of the system does occur on a much longer time scale of about 0.1 s. This slower process corresponds to the comproportionation of two relatively stable 18e$^-$ species, $W(CO)_5^{2-}$ and $W(CO)_5(CH_3CN)$, formed by the parallel metal–metal bond heterolysis, Eq. (4).

$$W_2(CO)_{10}^{2-} \xrightleftharpoons{h\nu} W(CO)_5^{2-} + W(CO)_5(CH_3CN) \tag{4}$$
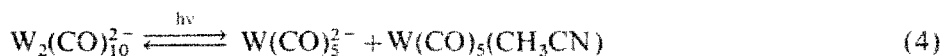
Photochemical heterolytic tungsten–osmium bond cleavage was recently reported for $(Me_3P)(OC)_4OsW(CO)_5$ [23].

3.2. Ion pairing and solvent effects

$[W_2(CO)_{10}]^{2-}$ would be expected to exhibit significant effects of ion pairing, especially in solvents with lower dielectric constants such as THF ($\epsilon = 7.6$), compared to CH_3CN ($\epsilon = 37.5$). Infrared spectroscopy is a straightforward method for evaluating ion pairing effects of metal carbonylates. For example, $Na_2[W_2(CO)_{10}]$ has $\nu(CO)$ bands at 1941(m), 1891(vs) and 1790(s) cm^{-1} in MeCN. These appear at 1945(m), 1903(vs) and 1753(m) cm^{-1} in THF. Addition of 18-crown-6 to a THF solution of $Na_2[W_2(CO)_{10}]$ results in an IR spectrum that is nearly identical to the spectrum in MeCN. Ion pairing is thus relatively strong in THF, but weaker in MeCN, and disrupted by the presence of the crown ether. In order to probe the effects of ion pairing, the bis(triphenylphosphine) iminium salt $[PPN]_2[W_2(CO)_{10}]$ compound was prepared. The IR spectrum of $[PPN]_2[W_2(CO)_{10}]$ in THF is spectroscopically similar to $Na_2[W_2(CO)_{10}]$ in MeCN, i.e. ion pairing is weak. Cyclic voltammograms of the $[PPN]_2[W_2(CO)_{10}]$ and $Na_2[W_2(CO)_{10}]$ salts in THF are similar and the oxidation potentials were found to be -0.77 V vs. SCE and -0.66 V vs. SCE, respectively. It is easier to oxidize the PPN salt since it is stabilized less by ion pairing than the sodium salt. Ion pairing also affects the recombination rate of the tungsten radicals. In acetonitrile, the recombination rate constant for $W(CO)_5^{-\cdot}$ radicals photogenerated from $Na_2[W_2(CO)_{10}]$ is $k_r = 3 \times 10^9$ M^{-1} s^{-1} and is essentially the same for the PPN salt. In THF solution, the recombination rate constant for photogenerated $W(CO)_5^{-\cdot}$ radicals is higher for $[PPN]_2[W_2(CO)_{10}]$ ($k_r = 1 \times 10^8$ M^{-1} s^{-1}) than for $Na_2[W_2(CO)_{10}]$ ($k_r = 3 \times 10^7$ M^{-1} s^{-1}). The recombination rates, however, do not appear to be completely governed by ion pairing. The recombination rate constant for $W(CO)_5^{-\cdot}$ radicals generated from $Na_2[W_2(CO)_{10}]$ is an order of magnitude higher ($k_r = 3 \times 10^8$ M^{-1} s^{-1}) in 2-methyltetrahydrofuran than it is in THF. This suggests that both ion pairing and specific solvation can impede $W(CO)_5^{-\cdot}$ radical recombination. Studies of the recombination rates of some other metal carbonyls $[(\eta^5-C_5R_5)Cr(CO)_3]_2$ (R = H, Me) showed little or no solvent dependence [22,24].

3.3. Transient absorption spectra of 19e$^-$ solvent–$W(CO)_5^{-\cdot}$ radicals

Transient absorption spectroscopy in the IR was used to observe photogenerated $W(CO)_5^{-\cdot}$ radicals in the presence of donor solvents and ligands. The UV–vis transient absorption spectrum resulting from the photolysis of $[W_2(CO)_{10}]^{2-}$ in acetonitrile is presented in Fig. 3. Bleaching of the $d\pi$–σ^* absorption at ca. 430 nm and appearance of intense absorptions throughout the visible region with a broad maximum at ca. 470 nm are evident. Since the UV–vis TA spectrum was found to remain relatively featureless and rather insensitive to the presence of different solvents or donor ligands, IR TA spectroscopy became the method of choice to study $W(CO)_5^{-\cdot}$ radicals.

The IR transient absorption spectrum obtained at < 1 μs following the laser pulse
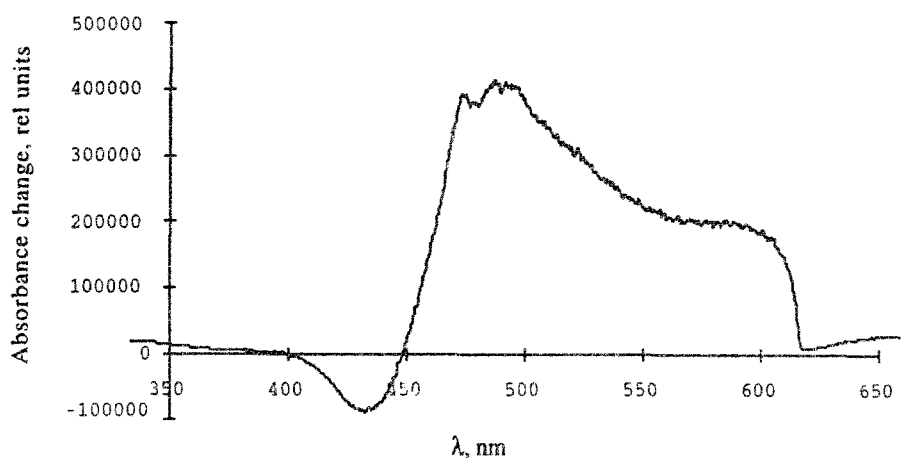
Fig. 3. Full transient absorption (TA) spectrum of $[W_2(CO)_{10}]^{2-}$ in the UV–vis region 10 μs after the laser pulse.

in MeCN is presented in Fig. 4. Soon after the laser pulse, the TA spectrum is dominated by new IR absorptions at $\nu(CO) > 1960 \, cm^{-1}$. These absorptions occur on average significantly higher in energy than those of $[W_2(CO)_{10}]^{2-}$. Thus, the relatively high energy absorptions would appear to correspond to free $W(CO)_5^{-\cdot}$ radicals formed by homolysis of $[W_2(CO)_{10}]^{2-}$. The decreased charge and number of electrons in the valence shell of a $W(CO)_5^{-\cdot}$ radical relative to $[W_2(CO)_{10}]^{2-}$ would be expected to raise the average energy of the $\nu(CO)$ bands in the free radical. In fact, low temperature matrix IR spectroscopic studies suggest the opposite. Burdett and Turner reported the infrared spectra of $M(CO)_5^{-\cdot}$ ($M = Cr$, Mo, W) radicals in matrices [25–27]. The $Cr(CO)_5^{-\cdot}$ radical anion was reported to exhibit a
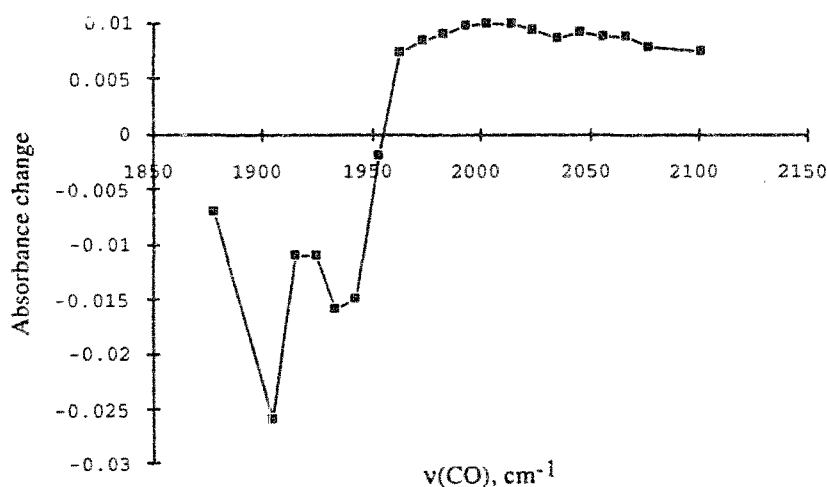

Fig. 4. Transient absorption (TA) spectrum of $[W_2(CO)_{10}]^{2-}$ in the IR region < 1 μs after the laser pulse.

strong doublet at 1857 and 1854 cm^{-1} and a single weaker band at 1840 cm^{-1} [26]. Identical spectra were also reported to be observed in samples formed either by condensation of alkali metal atoms into the matrix or by electron bombardment of a $Cr(CO)_6$/Ar matrix. The authors concluded that the IR spectral features at 1857, 1854 and 1840 cm^{-1} could not correspond to an ion paired species [26]. Although not reported explicitly, the infrared spectra of $W(CO)_5^{-\cdot}$ radicals were reported to be similar to the chromium case [26]. It is difficult to reconcile the IR TA spectrum observed at very short times with the low temperature matrix spectroscopic studies. It is possible that photochemical generation of $W(CO)_5^{-\cdot}$ radicals produces initially a species in a non-equilibrium (square pyramidal) geometry [26]. The IR transient absorption spectrum at longer times, however, changes dramatically. At times > 10 μs following the laser pulse, the TA spectrum is dominated by IR absorptions at $v(CO) = 1860$ and 1816 cm^{-1}, Fig. 5. Very similar shifts in the $v(CO)$ region to lower energy are observed after *ca.* 10 μs in THF or acetonitrile solvents. We conclude that the significant lowering of $v(CO)$ energy in the first 10 μs is assigned to a solvent–$W(CO)_5^{-\cdot}$ (solvent = THF, MeCN) radical. It is not immediately clear whether the low energy IR absorbing species formed after 10 μs is an authentic 19e$^-$ radical with the solvent molecule occupying the sixth coordination site, or the result of a less specific reorganization of the solvent shell. The higher energy features of the IR TA spectrum at longer times are strikingly close to those reported for $Cr(CO)_5^{-\cdot}$ radicals in matrices, but the lower energy band is some 30 cm^{-1} lower in energy. The > 1 μs rise time of the IR absorptions at $v(CO) = 1860$ and 1816 cm^{-1} suggests that the observed species is formed by a significantly activated process. Simon and coworkers have shown that formation of $Cr(CO)_5$(solvent) from photogenerated 16e$^-$ $Cr(CO)_5$ occurs on a picosecond timescale [28]. The markedly slower
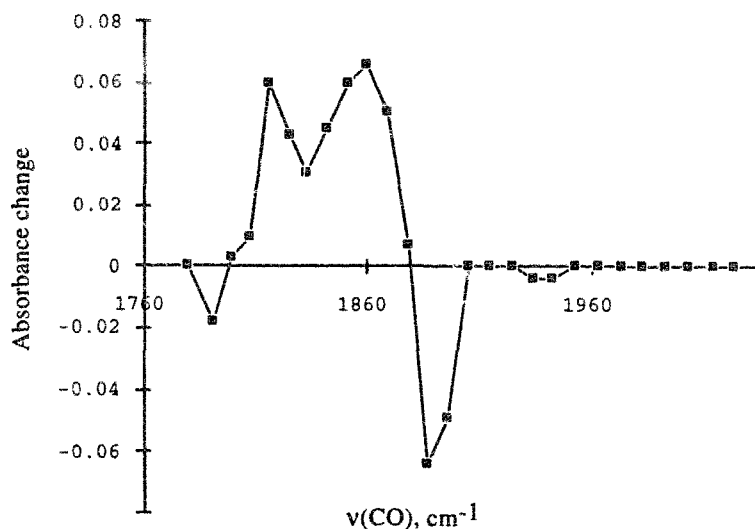

Fig. 5. Transient absorption (TA) spectrum of $[W_2(CO)_{10}]^{2-}$ in the IR region > 10 μs after the laser pulse.

process observed for $17e^-$ $W(CO)_5^-$ species is consistent with a significant barrier associated with the $17e^-/19e^-$ couple relative to the $16e^-/18e^-$ case (vide infra).

3.4. Electron transfers from photogenerated $19e^-$ solvent–$W(CO)_5^-$ radicals

One expected attribute of 19-valence electron radicals, such as [solvent–$W(CO)_5$]$^-$, is that they would be extremely potent reducing agents. We find that this is generally true. Substituted benzophenones (BP) were found to have sufficiently negative reduction potentials, $E^\circ(A/A^{-})$, to enable a systematic study of rates of electron transfer from photogenerated $[W(CO)_5(L)]^-$ to the benzophenone electron acceptors (A) as a function of thermodynamic driving force. Also, benzophenone radical anions have strong electronic absorptions in regions where $W(CO)_5^-$ radicals do not absorb significantly. Fig. 6 shows the monoexponential growth of transient absorption at 630 nm corresponding to the formation of the benzophenone radical anion (BP^-) when $[W_2(CO)_{10}]^{2-}$ is irradiated in the presence of benzophenone in THF solvent, under pseudo-first order conditions. This corresponds to the electron transfer process given in Eq. (5). The rate constant for the reduction of BP by $[W(CO)_5(THF)]^-$ is fast, $k_{et} = 6 \times 10^6$ M^{-1} s^{-1}, even though the reduction potential of BP is quite high, $E_{1/2}$ (BP/BP^{-}) = -1.91 V vs. SCE.

$$[W(CO)_5(THF)]^- + BP \xrightarrow{k_{et}} [W(CO)_5(THF)] + BP^- \qquad (5)$$
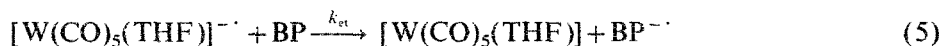
Before discussing the driving force dependence of rate constants for electron transfer from photogenerated $[W(CO)_5(L)]^-$ radicals in more detail, it is useful to estimate the oxidation potential of the $[W(CO)_5(L)]^-$ radicals. The reduction

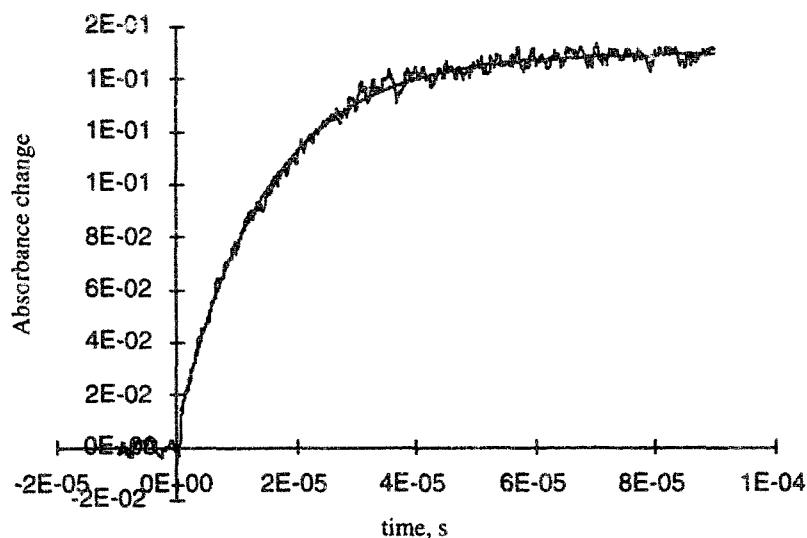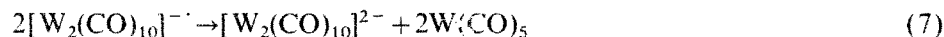Fig. 6. Appearance of benzophenone radical anion (BP^-) observed at 630 nm following laser excitation of $[W_2(CO)_{10}]^{2-}$ and benzophenone (BP) in THF.

potential of $W(CO)_6$ has been reported variously to be between -2.6 V [29] and -2.04 V [30] vs. SCE. However, we find electrochemical reduction of $W(CO)_6$ to be completely irreversible even at scan rates up to 100 V s^{-1} with $E_{p,c}$ at -2.0 V vs. SCE. Electrochemical reduction of $Cr(CO)_6$ appears very much like that of $W(CO)_6$ and is reported to be irreversible at scan rates up to 10^4 V s^{-1} with $E_{p,c}$ at *ca.* -2 V vs. SCE [31]. Similarly, for $W(CO)_5(THF)$ we find that the electrochemical reduction is irreversible at scan rates up to 100 V s^{-1} and occurs approximately 100 mV more cathodic than $W(CO)_6$. Electrochemical reductions of $W(CO)_5(DMF)$, $W(CO)_5(PC)$ (where DMF = dimethylformamide; PC = propylene carbonate) and $W(CO)_5(CH_3CN)$ were found to be irreversible but are observed at potentials anodic compared to $W(CO)_6$ [30]. We conclude that the thermodynamic potential for the $W(CO)_5(THF)/W(CO)_5(THF)^-$ couple can only be estimated at this point. Tyler assumes that substitution of one CO ligand by trimethylphosphine shifts the oxidation potential by *ca.* 0.5 V more cathodic [7]. On this basis, he estimates the oxidation potential of $W(CO)_5(PEt_3)^{-\cdot}$ species as -3.1 V vs. SCE (i.e. similar to that of sodium metal in aqueous solution, $E^\circ = -2.95$ V vs. SCE [32]). This is probably an overestimate, but nonetheless a value *ca.* -2.9 V is not unreasonable. Hence, from a strictly thermodynamic consideration, photogenerated $[W(CO)_5(L)]^{-\cdot}$ radicals should be capable of reducing almost anything. However, the useful range is limited by the oxidation potential of $Na_2[W_2(CO)_{10}]$, which is itself a reasonably strong reductant, $E_{1/2}(W_2(CO)_{10}^{-\cdot}/W_2(CO)_{10}^{2-}) = -0.66$ V vs. SCE, or -0.77 V for the PPN salt. Thus, potential electron acceptors for electron transfers from photogenerated $[W(CO)_5(L)]^{-\cdot}$ radicals must have reduction potentials, $E^\circ(A/A^{-\cdot})$, at least as negative as -0.66 V vs. SCE. Otherwise, thermal reduction of the acceptor by the parent tungsten dimer will occur. However, the estimated potential of -0.66 V is a thermodynamic value, i.e. it is based on the assumption that Eq. (6) truly represents a thermodynamic equilibrium, which is almost certainly not the case.

$$[W_2(CO)_{10}]^{2-} + e^- \rightleftharpoons [W_2(CO)_{10}]^{-\cdot} \tag{6}$$

The oxidized species, $[W_2(CO)_{10}]^{-\cdot}$, has one electron removed from the bonding σ-orbital which sufficiently weakens the metal–metal bond such that a disproportionation reaction, Eq. (7), takes place followed by the extremely fast trapping of the 16e$^-$ $W(CO)_5$ species, Eq. (8) [33]:

$$2[W_2(CO)_{10}]^{-\cdot} \rightarrow [W_2(CO)_{10}]^{2-} + 2W(CO)_5 \tag{7}$$

$$W(CO)_5 + THF \rightarrow W(CO)_5(THF) \tag{8}$$

The measured rate constant of the disproportionation reaction, Eq. (7), is 2.5×10^3 M^{-1} s^{-1} [29]. This suggests that the effective thermodynamic potential (E°) is more negative than the measured $E_{1/2}$ value of -0.66 V vs. SCE. We observe that electron acceptors with reduction potentials positive of -1 V vs. SCE are reduced thermally by the tungsten dimer at an appreciable rate. The accessible range of reduction potentials, $E^\circ(A/A^{-\cdot})$, for electron acceptors with the $[W_2(CO)_{10}]^{2-}$ system is -2.9 to -1.0 V vs. SCE. We therefore focused on a series of substituted

benzophenones with reduction potentials spanning the range, $E_{1/2} = -2.3$ to -1.0 V vs. SCE.

Table 1 summarizes results of our studies of the kinetics of electron transfer from photogenerated $[W(CO)_5(THF)]^{-\cdot}$ radicals to a series of substituted benzophenone electron acceptors. A practical lower limit in measurable rate constant (due to the recombination of the tungsten radicals $[W(CO)_5(THF)]^{-\cdot}$), $k_{et} = 4 \times 10^4$ M^{-1} s^{-1}, was realized in the case of cyclohexylphenylketone with $E_{1/2} = -2.26$ V vs. SCE. Rate constants for electron transfer then increased over four orders of magnitude to an observed maximum, $k_{et} = 8 \times 10^8$ M^{-1} s^{-1}, for decafluorobenzophenone with $E_{1/2} = -1.21$ V vs. SCE. The presentation of $\log(k_{et})$ vs. $E_{1/2}$ $(A/A^{-\cdot})$ plot is striking and appears in Fig. 7. It is quite clear from Fig. 7 that a ceiling is imposed on the rates of electron transfer. Rate constants for electron transfers with nearly 1.8 V of driving force $(E_{1/2}$ $(W(CO)_5(L)^{0/-\cdot}) - E_{1/2}$ (decafluorobenzophenone$^{0/-\cdot}$) $\sim$

Table 1

Electron acceptor, A	k_{et} (M^{-1} s^{-1})[a]	$E_{1/2}$ $(A/A^{-\cdot})$[b]
Me2N—⬡—C(=O)—⬡—NMe2	Inner sphere	−2.26
Et2N—⬡—C(=O)—⬡—NEt2	Inner sphere	−2.28
⬡—C(=O)—⬡ (cyclohexyl phenyl)	4×10^4	−2.26
H3CO—⬡—C(=O)—⬡—OCH3	1×10^6	−2.14
H2N—⬡—C(=O)—⬡	8×10^5	−2.05
⬡—C(=O)—⬡	6×10^6	−1.91
Cl—⬡—C(=O)—⬡—Cl	2×10^7	−1.76
⬡—C(=O)—⬡—F5	3×10^7	−1.73
(CF3)⬡—C(=O)—⬡(CF3)	7×10^7	−1.60
F5—⬡—C(=O)—⬡—F5	8×10^8	−1.21
O2N—⬡—C(=O)—⬡	Dark	−1.05

[a] ±20% error; [b] V vs. SCE.
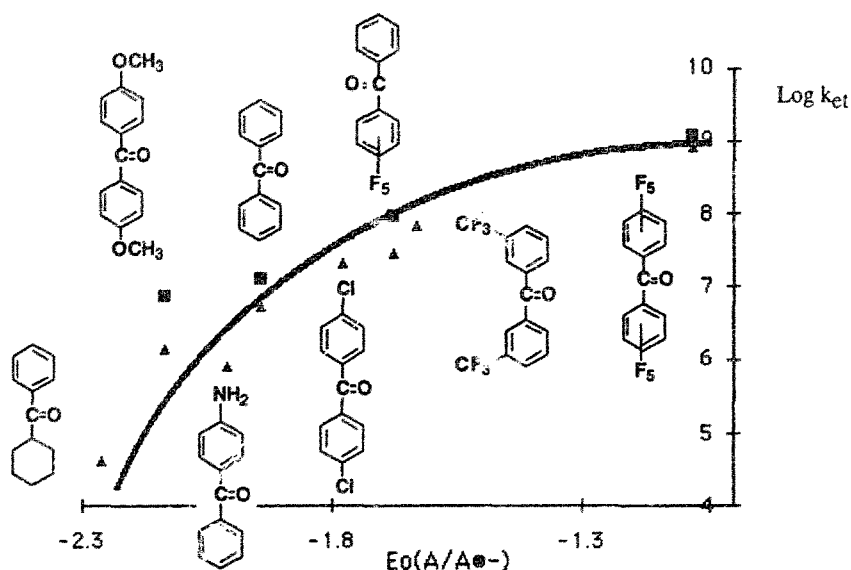
Fig. 7. Log(k_{et}) vs. E (A/A^{-}) for a series of benzophenone electron acceptors (A). Diamonds represent data taken in MeCN and triangles correspond to data in THF.

-1.8 V) fail to reach the diffusion controlled limit of *ca.* 10^{10} M^{-1} s^{-1}. We assume that the measured rate constant is the rate constant of the electron transfer step in the precursor complex, k_{et} in Eq. (9).

$$A + B^{-} \underset{k_{dc}}{\overset{k_{-dc}}{\rightleftharpoons}} AB^{-} \xrightarrow{k_{et}} \{AB^{-}\}^{\dagger} \rightarrow A^{-} + B \tag{9}$$
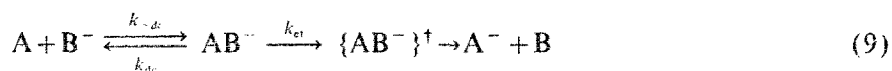
In this case, the classic Marcus expression for the rate constant, Eq. (10)

$$k_{obs} = \frac{k_{dc}}{1 + [(k_{dc})/(K_{DC})Z] \exp \{(\lambda/4RT)[1 + (\Delta G^{0}/\lambda)]^{2}\}} \tag{10}$$

becomes

$$k_{obs} = K_{DC} Z \exp \left[\frac{\lambda}{4RT} \left(1 + \frac{\Delta G^{0}}{\lambda} \right)^{2} \right] \tag{11}$$

where the diffusion-controlled rate constant k_{dc} is taken as 1.3×10 M^{-1} s^{-1} in THF and 2×10 M^{-1} s^{-1} in MeCN, and λ is the total reorganizational energy. K_{DC} is the equilibrium constant in Eq. (9). The driving force, ΔG^{0}, is calculated from the Rehm–Weller [34] relation Eq. (12).

$$\Delta G^{0} = -F[E_{red}^{0}(A/A^{-}) - E_{red}^{0}(D/D^{-})] \tag{12}$$

Since the exact oxidation potential of the nineteen electron tungsten species is not known, the experimental data must be fit to three unknown parameters: K_{DC}, λ and E^{0} (W(CO)$_{5}$(L)$^{0/-}$). In practice, the adjustable parameter that most affects the fit

of the experimental data is the total reorganization energy, λ. The experimental data and the best fit (for the data in THF) are depicted in Fig. 7. The data are essentially the same in acetonitrile and THF. The muted acceleration in rates of electron transfer from the photogenerated $W(CO)_5(L)^{-\cdot}$ radicals to the substituted benzophenones indicates a very high reorganizational energy, λ. Fig. 8 compares the effect of higher reorganization energies on rates of electron transfer (given by Eq. (11)) as a function of driving force, ΔG^0. The generally slow approach of rates of electron transfer to the limit of diffusion control for driving forces approaching 1.8 eV are expected for reorganization energies on the order of 3 eV. The best fit of our experimental data to Eq. (11) yields a value of $\lambda = 70$ kcal mol^{-1} (3.03 eV), $K_{DC} = 64$ M^{-1} L^{-1} and E^0 ($W(CO)_5(L)^{0/-\cdot}$) = -3.1 V vs. SCE. A large reorganization energy follows naturally from a large nuclear displacement in the reaction coordinate at any driving force. Fig. 9 shows how the barrier heights increase in the potential energy surface for a reaction with a larger nuclear displacement, compared to a smaller displacement at similar driving force. This is quite similar to studies of $Co^{II/III}$ electron transfer reactions reported by Endicott, where the bond length differences between the two oxidation states approach 0.2 Å, contributing to inner sphere reorganization energies on the order of 3 eV [35–37]. In one case, the X-ray structure of the genuine 19e$^-$ complex $CpFe(C_6Me_6)$ showed lengthening of the distance between the Fe center and the Cp ring by 0.1 Å compared to the corresponding 18e$^-$ species [2,14]. Bond lengthening between the tungsten center and the carbonyl ligands is estimated to be close to 0.2 Å.
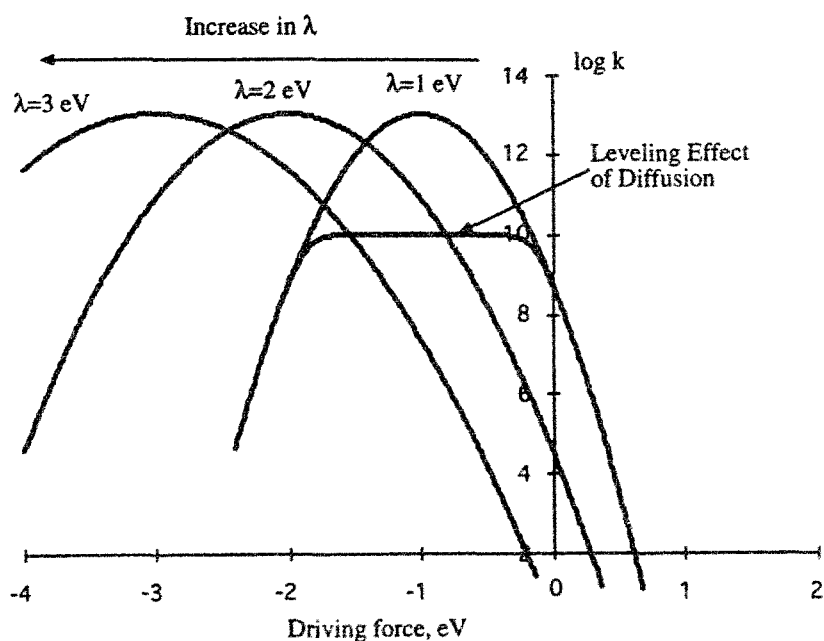

Fig. 8. The effect of higher reorganization energies (λ) on the rates of electron transfer (k_{et}) vs. driving force (ΔG^0) profiles predicted by the Marcus quadratic barrier relation.
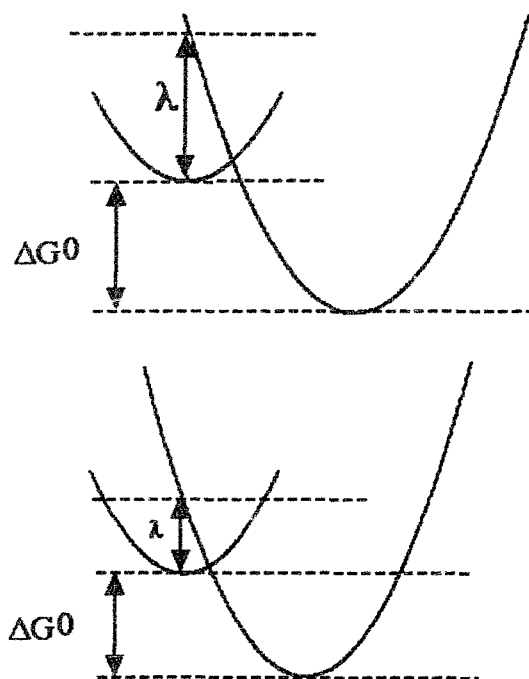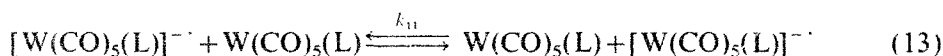
Fig. 9. Comparison of a potential energy surface for reactions with different nuclear displacement at similar driving force. ΔG^0.

Assuming the thermal barrier to the degenerate tungsten radical self-exchange, Eq. (13), is $\lambda/4$, the self-exchange rate constant, k_{11}, is predicted to be less than 1 $M^{-1} s^{-1}$.

$$[W(CO)_5(L)]^{-\cdot} + W(CO)_5(L) \xrightleftharpoons{k_{11}} W(CO)_5(L) + [W(CO)_5(L)]^{-\cdot} \qquad (13)$$

Scott and Espenson have shown that the self-exchange rate is very sensitive to the coordination of a solvent molecule [38]. They estimate a self-exchange rate constant of $5 \times 10^6 \, M^{-1} s^{-1}$ for the $CpW(CO)_3/CpW(CO)_3^-$ case and $5 \times 10^{-12} \, M^{-1} s^{-1}$ for the $CpW(CO)_3/CpW(CO)_3(solvent)^+$ case. Brown reports a reorganizational energy for $Re(CO)_4L^{\cdot+}/Re(CO)_4L^{\cdot}$ ($L = PMe_3$ or $P(O\text{-}i\text{-}Pr)_3$) to be $\lambda = 12 \, kcal \, mol^{-1}$ [39-42].

The abnormally large total reorganization energy, $\lambda = 70 \, kcal \, mol^{-1}$, and slow derived self-exchange rate constant $k_{11} < 1 \, M^{-1} s^{-1}$ for solvent–$W(CO)_5^{-\cdot}$ radicals reflect the large nuclear displacements associated with the $18e^-/19e^-$ couple. We conclude that although $19e-$ solvent–$W(CO)_5^{-\cdot}$ radicals are thermodynamically "super reducing agents", capable in principle of single electron transfers to a wide variety of electron acceptors, they are kinetically incompetent due to the enormous reorganization energy required to accommodate the nineteenth electron.
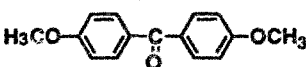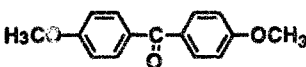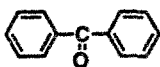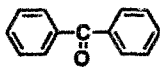
3.5. Effect of added nucleophiles on electron transfer reactivity and inapplicability of the radical chain mechanism

The irradiation of $[W_2(CO)_{10}]^{2-}$ in the presence of phosphine donor ligands, such as PPh_3 or PEt_3, leads to photochemical disproportionation, Eq. (14).

$$[W_2(CO)_{10}]^{2-} + PPh_3 \xrightarrow{h\nu} W(CO)_5(PPh_3) + [W(CO)_5]^{2-} \tag{14}$$
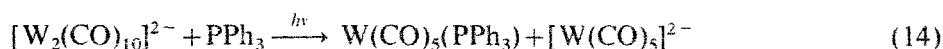
A surprising finding in our studies is that the presence of the alkylphosphines, even in large excess, only slightly increases rates of electron transfer to well defined benzophenone electron acceptors. Table 2 compares rate constants for electron transfer to benzophenone ($E_{1/2}$ (A/A$^{\cdot-}$) = -1.91 V vs. SCE) and 4,4'-dimethoxybenzophenone ($E_{1/2}$ (A/A$^{\cdot-}$) = -2.14 V vs. SCE) in the presence and absence of PEt_3. One would expect to see the strongest effect of added phosphine in the case of the acceptors which are most difficult to reduce. This is true. In the case of 4,4'-dimethoxybenzophenone, the rate of the electron transfer reaction doubles (from 1.4×10^6 to 2.8×10^6 M^{-1} s^{-1}) in the presence of the 0.1 M PEt_3. However, for benzophenone we do not see any rate acceleration within our experimental error (less than 20%). The explanation for this relatively moderate effect is participation of the solvent (THF or acetonitrile) as a nucleophilic ligand in competition with PEt_3. Surely, neither THF nor acetonitrile can compete with PEt_3 in nucleophilic strength. In terms of relative concentrations of PEt_3 (0.05M) and THF (11M), we can estimate that the $[W(CO)_5(PEt_3)]^{\cdot-}$ species are at least 1000 times more reactive (k_{et} is 1000 times greater) than the solvated $[W(CO)_5(THF)]^{\cdot-}$ species. The relative reactivity of the $[W(CO)_5(PEt_3)]^{\cdot-}$ radicals also depends on the nature of the phosphine, following the order $PEt_3 \sim PBu_3 \gg PPh_3$. This is a crucial result in support of an overall mechanism for electron transfer that involves the participation of a 19e$^-$ solvated $[W(CO)_5(THF)]^{\cdot-}$ species. It is also clear that if the electron transfer mechanism involved 17e$^-$ $[W(CO)_5]^{\cdot-}$ radicals, rather than 19e$^-$ $[W(CO)_5(THF)]^{\cdot-}$ species, then the rate of reduction would always be identical in

Table 2

Electron acceptor, A	[PEt$_3$] (M)	k_{et} (M^{-1} s^{-1})[a]	$E_{1/2}$ (A/A$^{\cdot-}$)[b]
H$_3$CO–⬡–C(O)–⬡–OCH$_3$	0	14×10^6	-2.14
H$_3$CO–⬡–C(O)–⬡–OCH$_3$	0.01	2.8×10^6	-2.14
⬡–C(O)–⬡	0	6×10^6	-1.91
⬡–C(O)–⬡	0.05	6×10^6	-1.91

[a] $\pm 20\%$ error; [b] V vs. SCE.

the presence and absence of the phosphine ligand, and it is not. Similarly, Espenson reports that the reducing ability of the photogenerated $CpW(CO)_3$ radicals is increased only slightly in the presence of the triphenylphosphine [24,38]. Tilset reports that the $19e^-$ $CpW(CO)_3(NCMe)^+$ species is a stronger reductant than the corresponding $17e^-$ $CpW(CO)_3^+$ radicals by *ca.* 1.4 V [43]. If a similar potential difference applies to our case, then the $19e^-$ species would participate in most of the electron transfer chemistry, even though present at concentrations a few orders of magnitude lower than the corresponding $17e^-$ species. Reported values of the formation constants of $19e^-$ species formed from $17e^-$ species can be larger than unity which, together with higher reactivities, allows them to be extremely competitive reductants [17,44–47].

One other mechanistic point pertains to the possible involvement of radical chain processes in electron transfers of photogenerated radicals. Radical chain mechanisms have been invoked widely in the explanation of mechanisms for the reactions of metal carbonyls (such as $Cp_2Fe_2(CO)_4$, $Mn_2(CO)_{10}$, $Co_2(CO)_8$, etc.) in the presence of nucleophiles [48]. The mechanism below (Eqs. (15)–(18)), involving the intermediacy of $19e^-$ $[W(CO)5(PPh3)]^{-\cdot}$, was suggested by Tyler [7].

$$[W_2(CO)_{10}]^{2-} \underset{}{\overset{h\nu}{\rightleftharpoons}} 2W(CO)_5^{-\cdot} \tag{15}$$

$$W(CO)_5^{-\cdot} + PPh_3 \underset{}{\overset{k_f}{\rightleftharpoons}} [W(CO)_5(PPh_3)]^{-\cdot} \tag{16}$$

$$[W(CO)_5(PPh_3)]^{-\cdot} + W(CO)_5^{-\cdot} \rightarrow W(CO)_5(PPh_3) + [W(CO)_5]^{2-} \tag{17}$$

$$[W(CO)_5(PPh_3)]^{-\cdot} + [W_2(CO)_{10}]^{2-} \rightarrow W(CO)_5(PPh_3)$$
$$+ [W(CO)_5]^{2-} + W(CO)_5^{-\cdot} \tag{18}$$
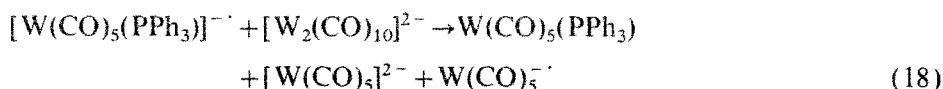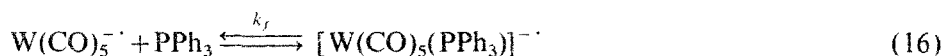
In the present study, we see no evidence for a radical chain mechanism. We have not found conditions where $Na_2[W_2(CO)_{10}]$ can be reduced by an electron transfer in THF solution. In electrochemical experiments, we do not observe any cathodic current due to the reduction of $Na_2[W_2(CO)_{10}]$ at potentials as far negative as -2.9 V vs. SCE (solvent/supporting electrolyte limit). We conclude that the driving force for reduction of $Na_2[W_2(CO)_{10}]$ by photogenerated $[W(CO)_5(PPh_3)]^{-\cdot}$ would be so low as to preclude a reaction in the presence of other electron acceptors.

4. Conclusions

Photochemical excitation of $[W_2(CO)_{10}]^{2-}$ leads to metal–metal bond homolysis and the formation of $W(CO)_5^{-\cdot}$ radicals. The premise that photogenerated $W(CO)_5^{-\cdot}$ radicals react with donor solvents or phosphine ligands (L = THF, MeCN, 2-methyl THF, PEt_3) to yield highly reducing $19e^-$ L–$W(CO)_5^{-\cdot}$ radicals was investigated by laser transient absorption spectroscopy in the UV–vis and IR regions and by electron transfer kinetics studies. The IR transient absorption spectrum at <1 μs

following the laser pulse in THF is dominated by new IR absorptions at $v(CO) > 1960$ cm^{-1}. The IR transient absorption spectrum at > 10 µs following the laser pulse is dominated by IR absorptions at $v(CO) = 1860$ and 1816 cm^{-1}. The significant lowering of $v(CO)$ energy in the first 10 µs is assigned to a solvated 19e$^-$ THF–W(CO)$_5^-$ $\cdot$ radical. A homologous series of substituted benzophenone electron acceptors (A) with $E_{1/2}$ (A/A$^-$) ranging from -1.21 to -2.26 V vs. SCE were used in a study of the electron transfer chemistry of the 19e$^-$ species in THF and acetonitrile. Electron transfer rate constants (k_{et}) were found to range from 4×10^4 M^{-1} s^{-1} for reduction of the least energetically favorable acceptor (cyclohexylphenylketone, $E_{1/2} = -2.26$ V vs. SCE) up to 8×10^8 M^{-1} s^{-1} for reduction of the most energetically favorable acceptor (decaflurobenzophenone, $E_{1/2} = -1.21$ V vs. SCE). A key finding in this study is that in donor solvents such as THF and acetonitrile, rates of electron transfer to benzophenone electron acceptors are only modestly accelerated by the addition of PEt$_3$. This provides strong evidence for the direct involvement of solvent as a nucleophilic ligand in the formation of 19e$^-$ solvent–W(CO)$_5^-$ $\cdot$ radicals. Electron transfer data were interpreted within the context of the Marcus theory of electron transfer. An abnormally large total reorganization energy, $\lambda = 70$ kcal mol^{-1}, and slow derived self-exchange rate constant $k_{11} < 1$ M^{-1} s^{-1} reflect the large nuclear displacements associated with the 18e$^-$/19e$^-$ couple. The 19e$-$ solvent–W(CO)$_5^-$ $\cdot$ radicals provide a classic illustration of the power of a reducing agent being the product of current (electron transfer rate) and potential (thermodynamic reduction potential) for a system. In this case, the enormous thermodynamic potential of solvent–W(CO)$_5^-$ $\cdot$ radicals is not realized because of slow kinetics arising from the large bond length and solvent reorganizations required by the electron transfer.

Acknowledgements

References

[1] D.R. Tyler, Acc. Chem. Res. 24 (1991) 325.
[2] D. Astruc, Chem. Rev. 88 (1988) 1189.
[3] J.W. Hershberger, R.J. Klinger, J.K. Kochi, J. Am. Chem. Soc. 104 (1982) 3034.
[4] D.J. Kuchynka, C. Amatore, J.K. Kochi, Inorg. Chem. 25 (1986) 4087.
[5] D.R. Tyler, F. Mao, Coord. Chem. Rev. 97 (1990) 119.
[6] W.C. Trogler, in: W.C. Trogler (Ed.), Organometallic Radical Processes, Elsevier, New York, 1990.
[7] N.D. Silavwe, A.S. Goldman, R. Ritter, D.R. Tyler, Inorg. Chem. 28 (1989) 1231.

[8] A.E. Stiegman, D.R. Tyler, Coord. Chem. Rev. 63 (1985) 217.

[9] N.D. Silavwe, X. Pan, D.R. Tyler, Inorg. Chim. Acta 144 (1988) 123.

[10] J.P. Blaha, M.S. Wrighton, J. Am. Chem. Soc. 107 (1985) 2694.

[11] R.E. Dessy, F.E. Stary, R.B. King, M.J. Waldrop, J. Am. Chem. Soc. 88 (1966) 471.

[12] M.C.R. Symons, S.W. Brat, J.L. Wyatt, J. Chem Soc., Dalton Trans. (1982) 991.

[13] D. Astruc, J.R. Hamon, E. Roman, P.J. Michaud, J. Am. Chem. Soc. 103 (1981) 7502.

[14] D. Astruc, J.R. Hamon, G. Althoff, E. Roman, P. Batail, P.J. Michaud, J.P. Mariot, F. Varret, D.J. Cozak, J. Am. Chem. Soc. 101 (1979) 5445.

[15] A.J. Dixon S.J. Gravelle, L.J. Van de Burgt, M. Poliakoff, J.J. Turner, E. Weitz, J. Chem. Soc., Chem. Commun. (1987) 1023.

[16] J.C. Green, M.R. Kelly, M.P. Payne, E.A. Seddon, D. Astruc, J.R. Hamon, P. Michaud, Organometallics 2 (1983) 211.

[17] C.E. Philbin, C.A. Granatir, D.R. Tyler, Inorg. Chem. 25 (1986) 4807.

[18] R.A. Marcus, N. Sutin, Biochim. et Biophys. Acta 811 (1985) 265.

[19] J.R. Balton, N. Mataga, G. McLendon, in: Advances in Chemistry, vol. 228, ACS, Washington, DC, 1991.

[20] B. McNamara, D.M. Becher, M.H. Towns, E.R. Grant, J. Phys. Chem. 92 (1988) 1458.

[21] B. McNamara, E.R. Grant, J. Phys. Chem. 98 (1994) 4622.

[22] S.L. Scott, J.H. Espenson, Z. Zhu, J. Am. Chem. Soc. 115 (1993) 1789.

[23] J.L. Male, H.B. Davis, R.K. Pomeroy, D.R. Tyler, J. Am. Chem. Soc. 116 (1994) 9353.

[24] Q. Yao, A. Bakac, J.H. Espenson, Organometallics 12 (1993) 2010.

[25] J.K. Burdett, J. Chem. Soc., Chem. Commun. (1973) 763.

[26] P.A. Breeze, J.K. Burdett, J.J. Turner, Inorg. Chem. 20 (1981) 3369.

[27] P.A. Breeze, J.J. Turner, J. Organomet. Chem. 44 (1972) C7.

[28] J.D. Simon, Pure and Appl. Chem. 62 (1990) 2243.

[29] C.J. Pickett, D. Pletcher, J. Chem. Soc., Dalton Trans. (1975) 879.

[30] A. Seurat, P. Lemoine, M. Gross, Electrochim. Acta 23 (1978) 1219.

[31] C. Amatore, P.J. Krusic, S.U. Pedersen, J.N. Verpeaux, Organometallics 14 (1995) 640.

[32] P.W. Atkins, Physical Chemistry, W.H. Freeman, New York, 1994.

[33] J.R. Philipps, W.C. Trogler, Inorg. Chim. Acta '98199200 (1992) 633.

[34] D. Rehm, A. Weller, Isr. J. Chem. 8 (1970) 259.

[35] J.F. Endicott, K. Kumar, T. Ramasami, F.P. Rotzinger, in: S.J. Lippard (Ed.), Progress in Inorganic Chemistry, vol. 30, Wiley, New York, 1983, p 141.

[36] J.F. Endicott, B. Durham, K. Kumar, Inorg. Chem. 21 (1982) 2437.

[37] J.F. Endicott, B. Durham, M.D. Glick, T.J. Anderson, J.M. Kuszaj, W.G. Schmonsees, K.P. Balakrishnan, J. Am. Chem. Soc. 103 (1981) 1431.

[38] S.L. Scott, J.H. Espenson, W.J. Chen, Organometallics 12 (1993) 4077.

[39] M.R. Burke, T.L. Brown, J. Am. Chem. Soc. 111 (1989) 5185.

[40] K.-W. Lee, T.L. Brown, J. Am. Chem. Soc. 109 (1987) 3269.

[41] P. Rushman, T.L. Brown, J. Am. Chem. Soc. 109 (1987) 3632.

[42] T.L. Brown, R.J. Sullivan, in: M. Chanon, M. Juliard, J.C. Poite (Eds.), Paramagnetic Organometallic Species in Activation/Selectivity Catalysis NATO ASI Series C· Mathematical and Physical Sciences, vol. 257, Kluwer Academic Publishers, Dordrecht, 1989, p 187.

[43] M. Tilset, Inorg. Chem. 33 (1994) 3121.

[44] M.P. Castellani, D.R. Tyler, Organometallics 8 (1989) 2113.

[45] M. Therien, W.C. Trogler, J. Am. Chem. Soc. 109 (1987) 5127.

[46] Y. Zhang, D.K. Gosser, P.H. Rieger, D.A. Sweigart, J. Am. Chem. Soc. 113 (1991) 4062.

[47] J.K. Kochi, D.J. Kuchynke, Inorg. Chem. 28 (1989) 855.

[48] D. Astruc, Electron Transfer and Radical Processes in Transition-Metal Chemistry, VCH Publishers, New York, 1995.